ISOMAse
International Society of Ocean, Mechanical and Aerospace Scientists and Engineers

Journal of Ocean, Mechanical and Aerospace
-Science and Engineering-
30th July 2025. Vol.69 No.2

July 30, 2025

Numerical Study of Finite Element Analysis (FEA) of Stress and Deformation in Strainer

Muhammad Haiqal [a], Amnur Akhyan [a,*], Jupri Yanda Zaira [a], Roni Novison [a], Rifan Rianto [a] and Mohd Azahari bin Razali [b]

[a)] *Mechanical Engineering Study Program, Department of Industrial Technology, Politeknik Caltex Riau. Umban Sari Street (Patin) No. 1 Rumbai, Pekanbaru 28265, Riau, Indonesia*
[b)] *Faculty of Mechanical and Manufacturing Engineering, Universiti Tun Hussein Onn Malaysia Parit Raja, Batu Pahat, Johor, Malaysia*

*Corresponding author: akhyan@pcr.ac.id

Paper History

Received: 04-June-2025
Received in revised form: 10-July-2025
Accepted: 30-July-2025

ABSTRACT

Transportation of hydrocarbon gas in industry often carries contaminants such as scale, rust, and weld metal particles that can disrupt the flow and damage components such as compressors. Strainers are used to filter impurities before the fluid enters the main system. At high flow rates, strainers, especially perforated plates, are susceptible to structural damage. Because experimental tests are expensive and risky, Finite Element Analysis (FEA) simulations are used. This study analyzes the effect of variations in methane gas flow rates on the strength of carbon steel strainers with plate thicknesses of 0.8 mm, 1 mm, and 2 mm. The tested velocities were 7.59 m/s, 9.59 m/s, and 11.59 m/s at a pressure of 10 bars and a temperature of 55°C. The results showed the highest stress at the base of the strainer: 32,826 N/m^2 (0.8 mm), 30,472 N/m^2 (1 mm), and 21,975 N/m^2 (2 mm). The maximum deformations occurred at the strainer tip: 2.35×10^{-8} m, 2.91×10^{-8} m, and 2.82×10^{-8} m. All values are below the yield strength limit of carbon steel (2.5×10^{8}–5×10^{8} N/m^2), indicating a safe design against high flow loads.

KEYWORDS: *Hydrocarbon gas, Strainer, Von mises stress, Total deformation, FEA.*

NOMENCLATURE

σ_{vm}	Von mises stress
θ	Angle
s	Thickness
d	Hole diameter
D	Strainer diameter
τ_{xy}	Shear stress
L	Large

1.0 INTRODUCTION

Fluid distribution in the gas industry through piping systems often leads to damage in sensitive equipment, such as compressors [1],[2]. This damage is primarily caused by contaminants carried within the fluid, whether it is oil or gas [3]. Common contaminants include scale, rust, welding debris, and various other solid particles [4]. To mitigate compressor damage and thereby enhance oil and gas production, a filtration device known as a strainer is utilized [5]. A strainer is specifically designed to remove particulate matter from fluids before they enter sensitive components like compressors [6]. The use of strainers is expected to reduce maintenance frequency, lower maintenance costs, and minimize operational downtime. However, it is important to note that strainers can also alter fluid flow characteristic, including causing pressure drops [7].

In the oil and gas industry, strainers are commonly manufactured from carbon steel or stainless steel due to their durability and resistance to corrosion [6],[8]. The structural integrity of a strainer is a critical factor to consider, as inadequate strength can lead to mechanical failure [9]. Such failures may compromise the filtration efficiency [10], allowing contaminants to reach sensitive equipment like compressors. Potential damage to strainers includes cracks, deformation, and dents, all of which can impair their performance and reliability [11].

Other parameters that can influence the structural condition of a strainer include variations in strainer angle, hole diameter, and plate thickness. Previous studies have investigated various aspects of strainer design [6],[11]; however, the distinguishing factor in this study lies in the simulation parameters employed. These include plate thicknesses of 3 mm and 5 mm, a strainer angle of 81.35°, and

JOMAse | Received: 04-June-2025 | Accepted: 30-July-2025 | [(69) 2: 168-177]
Published by International Society of Ocean, Mechanical and Aerospace Scientists and Engineers, www.isomase.org., ISSN: 2354-7065 & e-ISSN: 2527-6085

the use of different fluid types.

The limited number of references on the structural performance of strainers, combined with the various challenges associated with experimental studies, makes numerical analysis the preferred approach. Several factors hinder the feasibility of experimental testing, including the high cost of acquiring components such as large-diameter pipes and strainers, the need for high fluid flow rates, and the use of hydrocarbon gases [12],[13]. Hydrocarbon gases pose significant risks due to their explosive, flammable [14], and hazardous nature [15]. Furthermore, experimental setups require gas storage tanks and strict safety measures to ensure the secure distribution of hydrocarbon gases [16],[17].

Due to the significant challenges and limitations associated with experimental testing of strainers, numerical simulation has emerged as a practical and effective alternative [18],[19]. In analyzing strainers, various modeling approaches have been employed, including Finite Element Analysis (FEA), which is widely used to evaluate the structural performance and validate the feasibility of strainer designs [6],[20]. Numerical analysis enables detailed evaluation of stress, strain, deformation, and other structural behaviors, facilitating design optimization and enhancing the overall safety and reliability of strainers [21].

In this study, structural analysis of a strainer design was performed using Finite Element Analysis (FEA) [22]. Numerical simulations were carried out to determine stress and deformation responses, highlighting the importance of design optimization and structural safety in strainers [23]. The objective of this study is to investigate the effects of variations in strainer plate thickness (0.8 mm, 1 mm, and 2 mm) and fluid flow velocity on the resulting stress and structural deformation in carbon steel strainers. The primary focus is to identify the locations of maximum stress concentration and peak deformation within the strainer structure, as well as to evaluate whether the design remains within safe material limits under specified flow conditions. The findings of this study are expected to serve as a reference for designing industrial strainers that are structurally stronger, more efficient, and safer under high-flow conditions.

2.0 METHODS

In this study, the test geometry was designed based on parameters and specifications relevant to the hydrocarbon gas industry [24], as outlined in Table 1. The test material used is carbon steel with a straight hole pattern [25],[26]. According to previous research [27], the pressure drop (ΔP) across a straight hole configuration is higher compared to a staggered hole configuration, resulting in a greater structural load on the strainer with a straight hole pattern.

Table 1: Strainer test geometry specifications [28]

D (Inch)	d (mm)	*Pitch* (mm)	s (mm)	L (mm)
6	4	6	0.8, 1 and 2	432

Based on these specifications, three strainer test geometries were developed, corresponding to three variations in plate thickness, as illustrated in Figure 1.

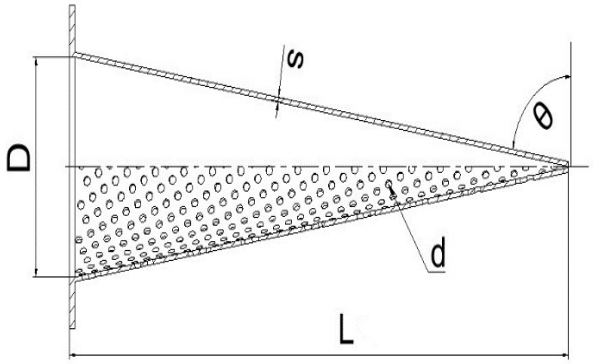

Symbol	Information
L	Large
D	Diameter
θ	Angle
s	Thickness
d	Hole Diameter

Figure 1: Strainer geometry [6]

2.1 Fluid Regions [29]

In areas containing fluid, flow simulation calculates the Navier Stokes equations, which describe the principles of conservation of mass, momentum, and energy.

$$\nabla \bar{u} = 0 \quad (1)$$

$$-\nabla P + \left(\mu + \rho\frac{k}{\omega}\right)\nabla^2 \bar{u} + \rho g = \rho\left(\frac{\partial \bar{u}}{\partial t} + \bar{u}.\nabla \bar{u}\right) \quad (2)$$

$$-\nabla P + \left(\mu + \rho\frac{k}{\omega}\right)\nabla^2 v + \rho g = \rho\left(\frac{\partial v}{\partial t} + v.\nabla v\right) \quad (3)$$

$$-\nabla P + \left(\mu + \rho\frac{k}{\omega}\right)\nabla^2 w + \rho g = \rho\left(\frac{\partial u}{\partial t} + w.\nabla w\right) \quad (4)$$

In flow simulation, the transport equation is used to determine the turbulent kinetic energy and its dissipation rate, by applying the k-omega model. The modified k-omega turbulence model with the damping function of Lam and Bremhorst (1981), which is used to describe laminar, turbulent, and transitional flow in homogeneous fluids, is based on the following turbulence conservation law:

$$\frac{\partial(\rho k)}{\partial t} + \nabla.(\rho U k) = \nabla.\left[\left(\mu + \frac{\mu t}{\sigma k}\right)\nabla k\right] + P_k + P_b - \rho\varepsilon + S_k \quad (5)$$

$$\frac{\partial(\rho\omega)}{\partial t} + \nabla.(\rho U\omega) = \nabla.\left(\left(\mu + \frac{\mu_t}{\sigma_k}\right)\nabla\omega\right) + \frac{\gamma}{v_t}P_k - \beta\rho\omega^2 \quad (6)$$

2.2 Von Mises Stress

Von Mises stress, also known as equivalent stress, represents a combined measure of multiple stress components acting on a material [30]. In the strainer, von Mises stress arises from the fluid pressure exerted on the strainer walls. This interaction between the fluid flow and the structure is commonly referred to as Fluid-Structure Interaction (FSI) [31].

JOMAse | Received: 04-June-2025 | Accepted: 30-July-2025 | [(69) 2: 168-177]
Published by International Society of Ocean, Mechanical and Aerospace Scientists and Engineers, www.isomase.org., ISSN: 2354-7065 & e-ISSN: 2527-6085

$$\sigma_{vm} = \sqrt{\frac{1}{2}[(\sigma_x - \sigma_y)^2 + 3(\tau_{xy})^2]} \quad (7)$$

Information:
σ_{vm}: *Von Mises Stress*
σ_x : Bending Stress on the x – Axis
σ_y : Bending Stress on the y – Axis
τ_{xy} : Shear Stress

2.3 Simulation with FEA

In Figure 2 depicted the flowchart illustrates the stages of the data collection process in this study. It begins with creating the strainer test geometry based on the specified parameters, along with defining the flow domain representing the fluid flow path. This is followed by the fluid flow simulation stage using the Fluent solver, which includes meshing, setting boundary conditions, and assigning material properties. Upon completion, the flow simulation results are transferred to the static structural analysis stage to evaluate the strainer's structural response. This stage involves meshing, defining fixed supports, assigning material properties, applying pressure loads, and solving the model. Finally, the simulation results are analyzed to draw conclusion.

3.0 RESULT AND DISCUSSION

In this study, the structural resistance of the strainer is evaluated under pressure exerted by a fluid in the form of hydrocarbon gas (methane). A comparative analysis is conducted to examine the effect of varying plate thicknesses (0.8 mm, 1 mm, and 2 mm) under different flow velocities (7.59 m/s, 9.59 m/s, and 11.59 m/s).

3.1 Straight Type Strainer Results Plate Thickness 0.8 mm

The FEA simulation results for the strainer with a straight holes configuration and a plate thickness of 0.8 mm were evaluated under flow velocities of 7.59 m/s, 9.59 m/s, and 11.59 m/s. The analysis focused on von Mises stress and total deformation to assess the structural response under varying flow conditions.

a. Velocity 7.59 m/s

As shown in Figure 3, the strainer with a straight hole configuration and a plate thickness of 0.8 mm undergoes deformation due to von Mises stress induced by a fluid flow velocity of 7.59 m/s. The highest stress concentration is observed at the bottom (base) of the strainer, with a value of 14,158 N/m², while the lowest stress occurs at the tip (outlet end) of the strainer, measuring 1.2245 N/m².

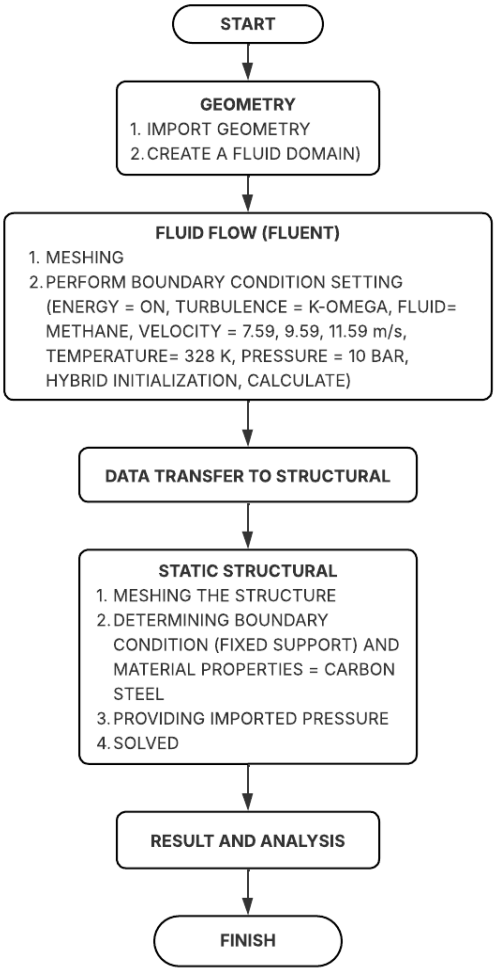

Figure 2: Data collection flowchart

JOMAse | Received: 04-June-2025 | Accepted: 30-July-2025 | [(69) 2: 168-177]
Published by International Society of Ocean, Mechanical and Aerospace Scientists and Engineers, www.isomase.org., ISSN: 2354-7065 & e-ISSN: 2527-6085

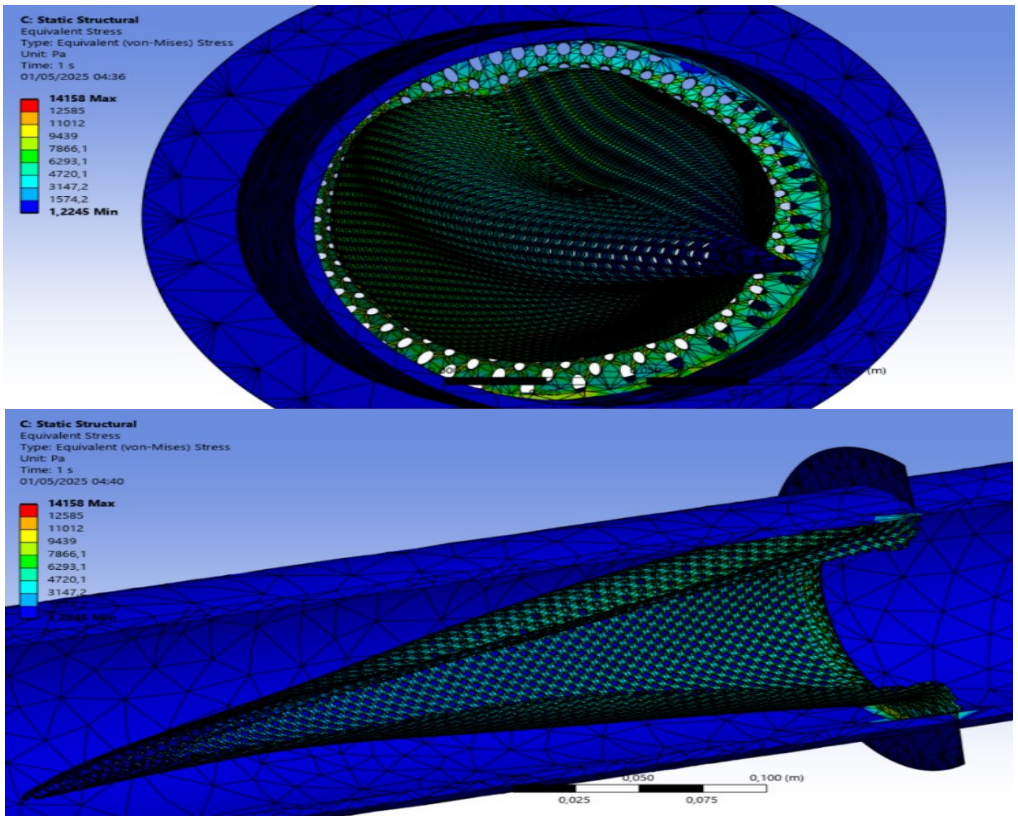

Figure 3: Von mises stress distribution on 0.8 mm thick strainer at 7.59 m/s flow velocity

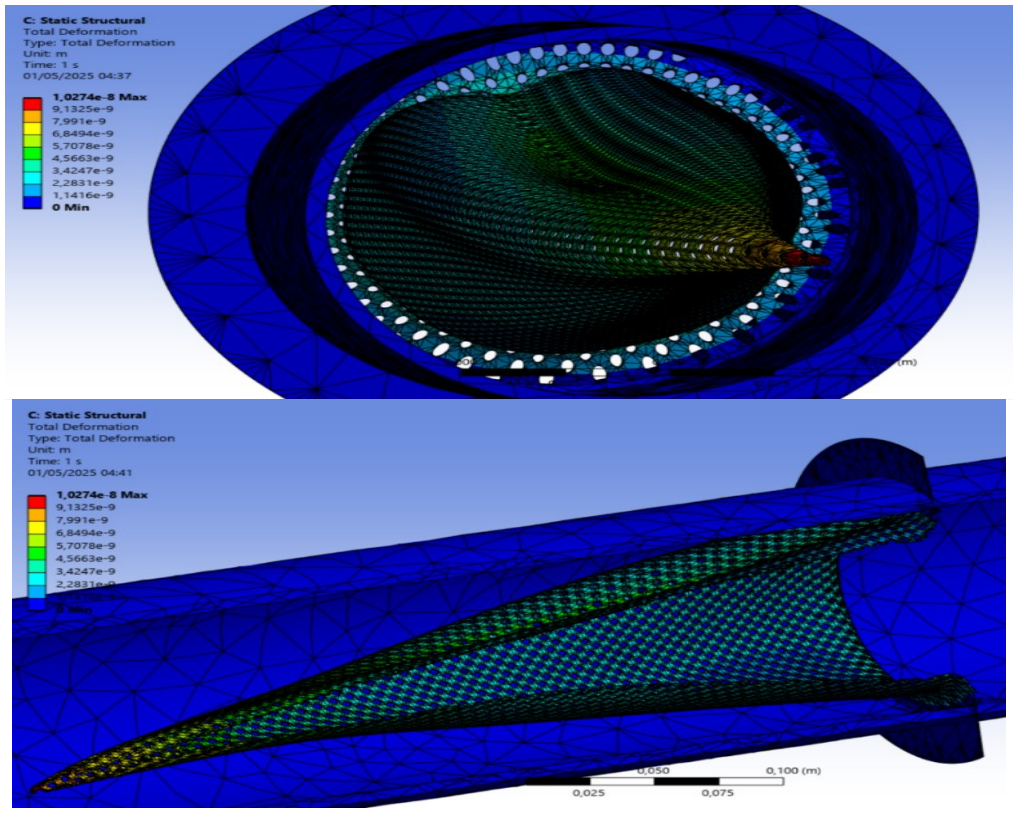

Figure 4: Total deformation result on 0.8 mm thick strainer at 7.59 m/s flow velocity

JOMAse | Received: 04-June-2025 | Accepted: 30-July-2025 | [(69) 2: 168-177]
Published by International Society of Ocean, Mechanical and Aerospace Scientists and Engineers, www.isomase.org., ISSN: 2354-7065 & e-ISSN: 2527-6085

As shown in Figure 4, the deformation results exhibit an inverse pattern relative to the stress distribution. The maximum deformation occurs at the tip (outlet end) of the strainer, with a value of 1.0274×10^{-8} m, while the minimum deformation is found at the base of the strainer, with a value of 1.1416×10^{-9} m.

Using the same method, the total deformation and von Mises stress results for flow velocities of 9.59 m/s and 11.59 m/s were obtained, as summarized in Table 2.

Table 2: Results of von Mises stress and total deformation of 0.8 mm plate strainer

Velocity (m/s)	Von Mises Stress (N/m^2)		Total Deformation (m)	
	Max	Min	Max	Min
7.59	14,158	1.2245	$1.0274x10^{-8}$	$1.1416x10^{-9}$
9.59	22,474	2.8878	$1.6241x10^{-8}$	$1.8045x10^{-9}$
11.59	32,826	2.7887	$2.3532x10^{-8}$	$2.6146x10^{-9}$

3.2 Straight Type Strainer Results Plate Thickness 1 mm

The FEA simulation results for the strainer with a straight hole configuration and a plate thickness of 1 mm were analyzed under flow velocities of 7.59 m/s, 9.59 m/s, and 11.59 m/s. The results include von Mises stress and total deformation, which reflect the structural response of the strainer under varying flow conditions.

a. Velocity 7.59 m/s

As shown in Figure 5, the strainer with a straight hole configuration and a plate thickness of 1 mm experiences deformation due to von Mises stress generated by a fluid flow velocity of 7.59 m/s. The highest stress concentration is observed at the bottom (base) of the strainer, with a value of 12,953 N/m², while the lowest stress occurs at the tip (outlet end) of the strainer, with a value of 2.28 N/m².

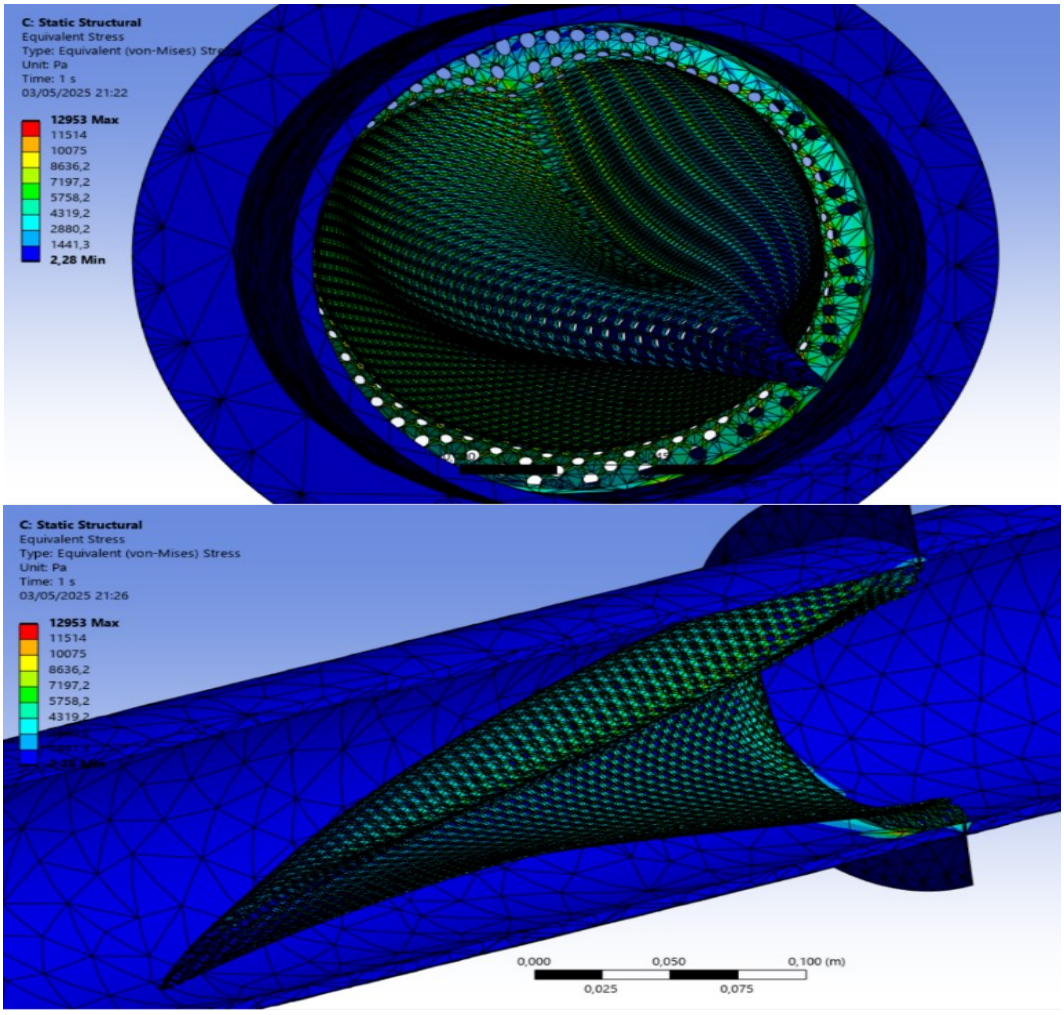

Figure 5: Figure 5: Von mises stress distribution on 1 mm thick strainer at 7.59 m/s flow velocity

JOMAse | Received: 04-June-2025 | Accepted: 30-July-2025 | [(69) 2: 168-177]
Published by International Society of Ocean, Mechanical and Aerospace Scientists and Engineers, www.isomase.org., ISSN: 2354-7065 & e-ISSN: 2527-6085

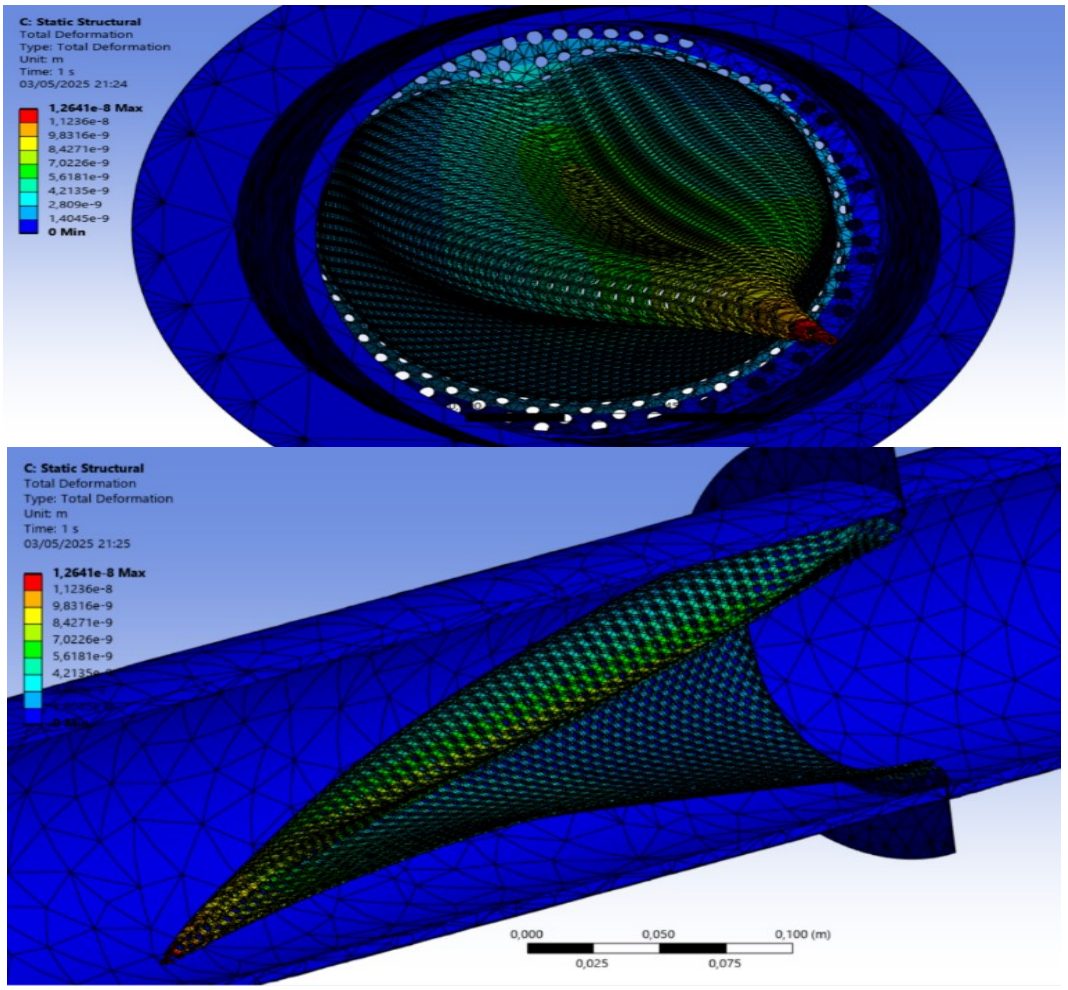

Figure 6: Total deformation result on 1 mm thick strainer at 7.59 m/s flow velocity

As shown in Figure 6, the deformation results display an inverse relationship to the stress distribution. The maximum deformation occurs at the tip (outlet end) of the strainer, with a value of 1.2641 × 10^{-8} m, while the minimum deformation is observed at the base of the strainer, with a value of 1.4045 × 10^{-9} m.

Using the same method, the total deformation and von Mises stress results for flow velocities of 9.59 m/s and 11.59 m/s were obtained, as summarized in Table 3.

3.3 Straight Type Strainer Results Plate Thickness 2 mm

The FEA simulation results for the strainer with a straight holes configuration and a plate thickness of 2 mm were analyzed under flow velocities of 7.59 m/s, 9.59 m/s, and 11.59 m/s. The results include von Mises stress and total deformation, which reflect the structural response of the strainer under varying flow conditions.

a. Velocity 7.59 m/s

As shown in Figure 7, the strainer with a straight hole configuration and a plate thickness of 2 mm experiences deformation due to von Mises stress induced by a fluid flow velocity of 7.59 m/s. The highest stress is concentrated at the bottom (base) of the strainer, with a value of 9,513.5 N/m², while the lowest stress occurs at the tip (outlet end) of the strainer, measuring 3.4532 N/m².

Table 3: Results of von Mises stress and total deformation of 1 mm plate strainer

Velocity (m/s)	Von Mises Stress (N/m^2)		Total Deformation (m)	
	Max	Min	Max	Min
7.59	12,953	2.2800	1.2641x10^{-8}	1.4045x10^{-9}
9.59	20,733	4.1644	1.992x10^{-8}	2.2133x10^{-9}
11.59	30,472	5.5468	2.9067x10^{-8}	3.2297x10^{-9}

JOMAse | Received: 04-June-2025 | Accepted: 30-July-2025 | [(69) 2: 168-177]
Published by International Society of Ocean, Mechanical and Aerospace Scientists and Engineers, www.isomase.org., ISSN: 2354-7065 & e-ISSN: 2527-6085

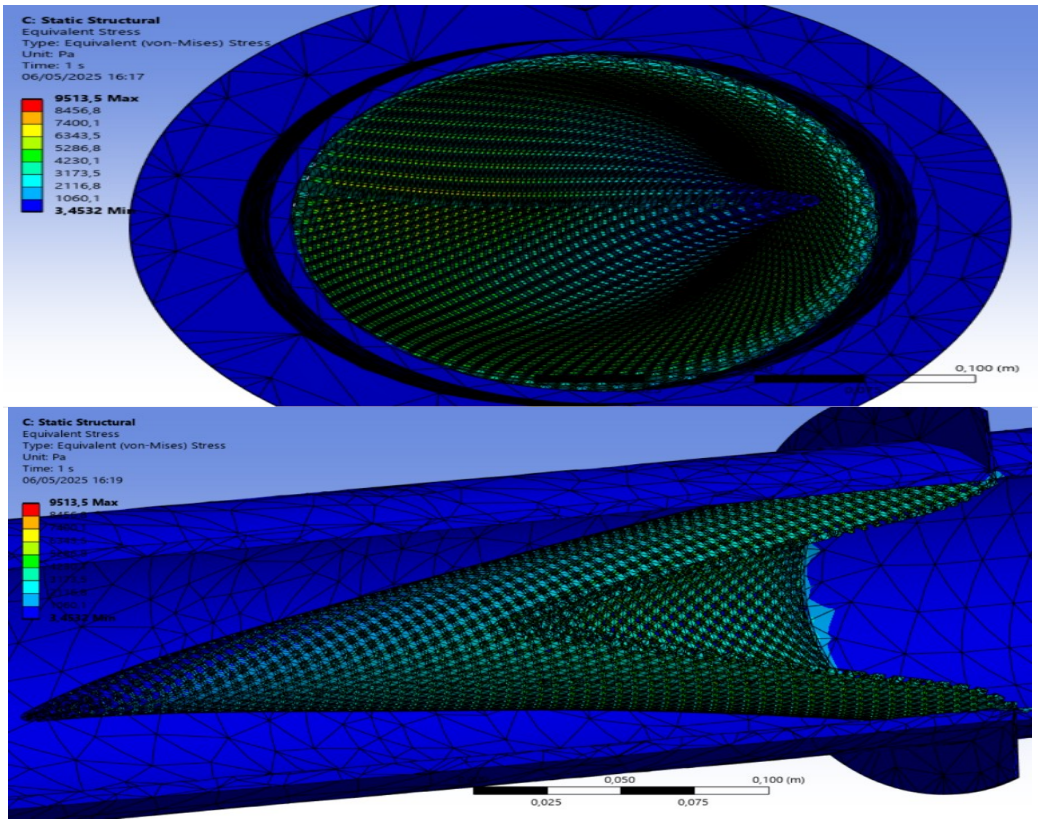

Figure 7: Von mises stress distribution on 2 mm thick strainer at 7.59 m/s flow velocity

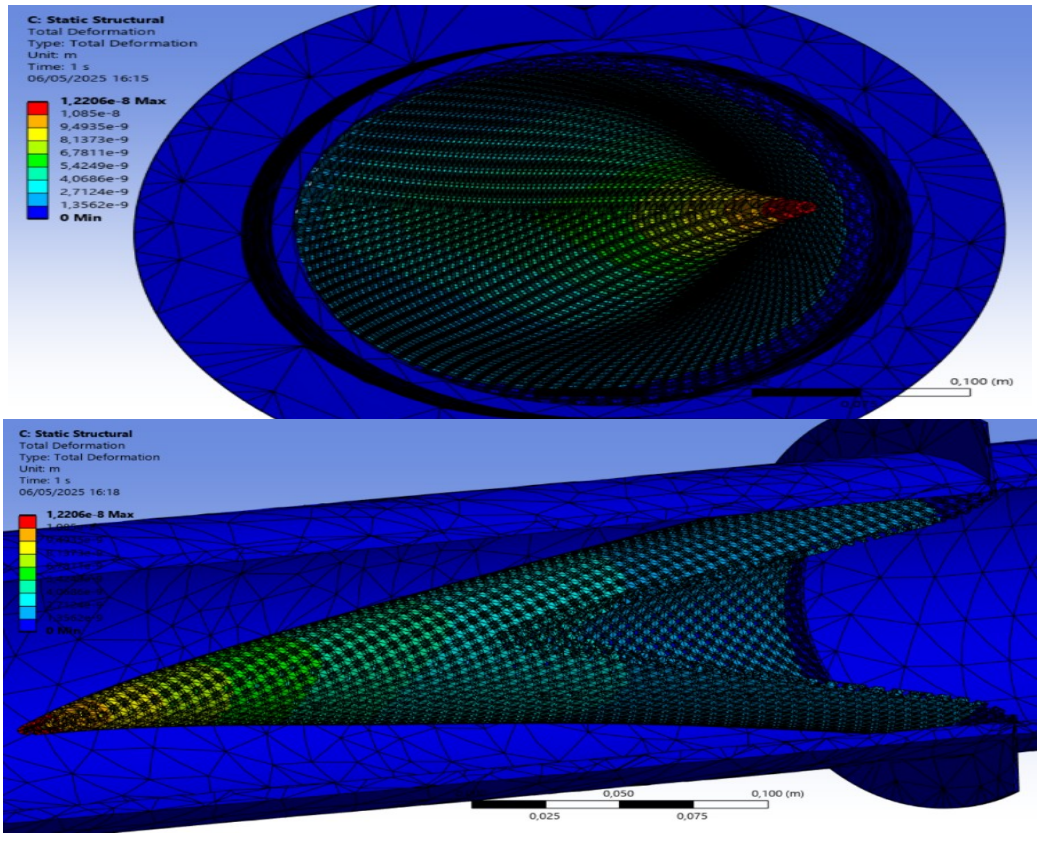

Figure 8: Total deformation result on 2 mm thick strainer at 7.59 m/s flow velocity

JOMAse | Received: 04-June-2025 | Accepted: 30-July-2025 | [(69) 2: 168-177]
Published by International Society of Ocean, Mechanical and Aerospace Scientists and Engineers, www.isomase.org., ISSN: 2354-7065 & e-ISSN: 2527-6085

As shown in Figure 8, the deformation results exhibit an inverse relationship to the stress distribution. The maximum deformation occurs at the tip (outlet end) of the strainer, with a value of 1.2206 × 10^{-8} m, while the minimum deformation is observed at the base of the strainer, with a value of 1.3562 × 10^{-9} m.

Using the same method, the total deformation and von Mises stress results for flow velocities of 9.59 m/s and 11.59 m/s were obtained, as summarized in Table 4.

Figure 9 presents the relationship between fluid flow velocity and von Mises stress on strainers with varying plate thicknesses of 2 mm, 1 mm, and 0.8 mm. It is evident that von Mises stress increases with higher flow velocities. Additionally, plate thickness significantly influences the magnitude of stress; the thinner plate (0.8 mm) experiences higher stress levels compared to the thicker plate (2 mm). At the highest velocity of 11.59 m/s, the stress reaches 32,826 N/m² for the 0.8 mm plate. These results highlight the critical role of plate thickness in resisting fluid pressure loads, which intensify as flow velocity increases.

Figure 10 illustrates the relationship between fluid flow velocity and total deformation in strainers with plate thicknesses of 2 mm, 1 mm, and 0.8 mm. The graph indicates that total deformation increases with rising flow velocity. Notably, the highest deformation occurs in the strainer with a 1 mm plate thickness, reaching up to 2.91 × 10^{-8} m at a velocity of 11.59 m/s. Conversely, the thickest plate (2 mm) exhibits the lowest deformation. These results demonstrate that material thickness plays a crucial role in resisting deformation under increasing fluid load conditions.

Table 4: Results of von Mises stress and total deformation of 2 mm plate strainer

Velocity (m/s)	Von Mises Stress (N/m^2)		Total Deformation (m)	
	Max	Min	Max	Min
7.59	9,513.5	3.4532	1.2206x10^{-8}	1.3562x10^{-9}
9.59	15,119	5.3255	1.9463x10^{-8}	2.1626x10^{-9}
11.59	21,975	7.439	2.8229x10^{-8}	3.1365x10^{-9}

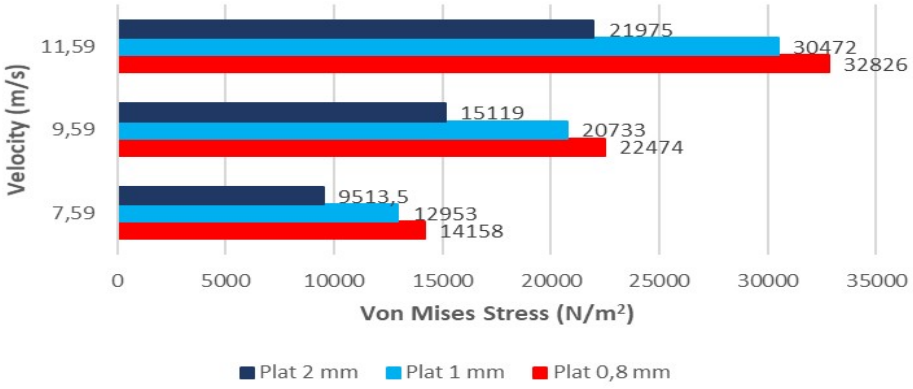

Figure 9: Velocity vs Von mises stress

Figure 10: Velocity vs Total deformation

JOMAse | Received: 04-June-2025 | Accepted: 30-July-2025 | [(69) 2: 168-177]
Published by International Society of Ocean, Mechanical and Aerospace Scientists and Engineers, www.isomase.org., ISSN: 2354-7065 & e-ISSN: 2527-6085

Figure 9 and Figure 10 show that the fluid flow velocity and plate thickness have a significant effect on the von Mises stress and total deformation of the strainer.

In Figure 9 illustrates that as the flow velocity increases, the von Mises stress also rises. The 0.8 mm plate experiences the highest stress of 32,826 N/m² at a velocity of 11.59 m/s, whereas the 2 mm plate only reaches 21,975 N/m². Figure 10 shows a similar trend in deformation. The maximum deformation occurs in the 1 mm plate at 2.91×10^{-8} m, while the 2 mm plate exhibits a deformation of only 2.82×10^{-8} m at the highest velocity. These results indicate that thinner plates tend to experience greater stress and deformation concentrations due to their limited capacity to withstand fluid flow loads. Compared to the findings in studies [32,33], this increase in stress and deformation in thinner plates aligns with fundamental material strength theory, where a reduction in material thickness decreases the moment of inertia, making the structure more susceptible to elastic and plastic deformation. The technical implication is that plate design in high-velocity fluid flow systems must consider a minimum thickness to prevent structural failure.

The simulation results indicate that the highest von Mises stress occurs at the bottom or base of the strainer, where the fluid pressure load is greatest. Conversely, the total deformation exhibits an opposite trend, with the maximum deformation occurring at the tip of the strainer and the minimum deformation at its base. After validation, these results and phenomena are consistent with similar studies conducted by [6]. Therefore, selecting the appropriate plate thickness is crucial in strainer design to maintain structural integrity against fluid pressure and velocity.

4.0 CONCLUSION

Based on the Finite Element Analysis (FEA) simulation conducted on a 6-inch strainer with a straight-hole pattern and plate thickness variations of 0.8 mm, 1 mm, and 2 mm, the following conclusions can be drawn: This study demonstrates that the structural performance of the strainer under varying fluid flow velocities is significantly influenced by plate thickness. Thinner plates exhibit higher stress and deformation concentrations, making them more susceptible to structural failure due to their reduced capacity to withstand fluid-induced loads. The location of maximum von Mises stress at the base of the strainer and maximum deformation at its tip identifies critical zones that require special attention in the design process. These findings are consistent with fundamental principles of material strength and are supported by previous research, emphasizing the importance of selecting a minimum plate thickness to maintain adequate structural integrity. For future strainer designs operating under high-velocity fluid flow conditions, engineers should prioritize optimizing plate thickness to achieve a balance between durability and material efficiency, thereby preventing premature failure and improving operational safety. Among the tested configurations, the 2 mm plate demonstrates superior structural response compared to the 0.8 mm and 1 mm plates. However, all thickness variations remain within safe limits, as the maximum stresses observed are well below the yield strength of carbon steel, which ranges from 2.5×10^8 - 5×10^8 N/m². Therefore, the strainer design used in this study is deemed structurally feasible and safe against potential failure.

ACKNOWLEDGEMENTS

First of all, the author would like to say Alhamdulillah for all the convenience and sustenance that has been given by Allah Subhanahuwata'ala, so that the author was able to complete this research. The author would like to express his deepest gratitude to my father Musfar and my mother Widya Ningsih who have prayed endlessly, as well as Mr. Amnur Akhyan, S.S.T., M.T., for his invaluable guidance and support as supervisor.

REFERENCES

[1] Deng, Y., Wang, X., Xu, J., Li, Y., Zhang, Y. & Kuang, C. (2022). Gas–liquid interaction characteristics in a multiphase pump under different working conditions. *Processes, 10*(10). https://doi.org/10.3390/pr10101977.

[2] Sotoodeh, K. (2023). The mathematical analysis and review of water hammering in check valves in offshore industry. *Journal of the Institution of Engineers (India): Series C, 104*(4), 879–885. https://doi.org/10.1007/s40032-023-00965-6.

[3] Wood, R.J.K. & Lu, P. (2021, June 1). Leading edge topography of blades-a critical review. *IOP Publishing Ltd*. https://doi.org/10.1088/2051-672X/abf81f.

[4] Sun, M., Cui, W. & Lin, N. (2023). Corrosion mechanism of typical shale gas gathering and transportation pipelines in Southwest China. *Journal of Physics: Conference Series, Institute of Physics*. https://doi.org/10.1088/1742-6596/2566/1/012106.

[5] Sotoodeh, K. (2019). Handling the pressure drop in strainers. *Marine Systems and Ocean Technology, 14*(4), 220–226. https://doi.org/10.1007/s40868-019-00063-2.

[6] Carlomagno, M., Rossin, S., Delvecchio, M. & Anichini, A. (2012). *Experimental and numerical validation of conical strainer fluid/structural performance model*. http://www.asme.org/about-asme/terms-of-use.

[7] Mahajan, G.P. & Maurya, R.S. (2020). *Development of an efficient T-type strainer with its performance evaluation*. Yildiz Technical University Press.

[8] Li, Z., Wang, Z., Liang, B. & Wang, X. (2024). Experimental study on hydrodynamic performance and structural forces of curved and vertical front face pile-supported permeable breakwaters. *Physics of Fluids, 36*(11). https://doi.org/10.1063/5.0237833.

[9] Haber, L.C. & Smith, J.M. (2012). Air ingestion and transport testing in a rotating drum raw water strainer. https://doi.org/10.1115/icone20-power2012-55231.

[10] Brnic, J., Krscanski, S., & Brcic, M. (2021). Comparison of responses of different types of steel alloys under the same loading and environmental conditions. *Proceedings of the Institution of Mechanical Engineers, Part L: Journal of Materials: Design and Applications*, *235*(6), 1194-1202.

[11] Motriuk, R.W. (2003). *A perforated conical strainer as*

an example of an acoustic noise generator. http://www.asme.org/about-asme/terms-of-use.

[12] Kementerian Energi dan Sumber Daya Mineral. (2013). *Direktorat Jenderal Minyak dan Gas Bumi*.

[13] Husnayain, F., Budiyanto, A., & Jufri, F. H. (2020). Studi Teknis Genset Termodifikasi Menggunakan Gas Alam dengan Variasi Tekanan Masukan. *Jurnal Nasional Teknik Elektro dan Teknologi Informasi*, *9*(3), 319-325.

[14] Nuur Darmawan, I., Kholistianingsih, Noor Fatah, A., Yulianto, P. & Adhi Pramono, S. (2023). Analisis methane gas detector dengan sensor catalytic dan sensor infrared di maintenance area II PT Kilang Pertamina Internasional RU IV Cilacap. *J-Proteksion: Jurnal Kajian Ilmiah Dan Teknologi Teknik Mesin*, *8*(1), 53–63. https://doi.org/10.32528/jp.v8i1.726.

[15] Ratih Andhika A.R, Yulia Lanti R.D. & Setyono, P. (2015). Pengaruh paparan gas metana (ch4), karbon dioksida (co2) dan hidrogen sulfida (h2s) terhadap keluhan gangguan pernapasan pemulung di tempat pembuangan akhir (tpa) sampah klotok kota Kediri. *Jurnal EKOSAINS, 7(2)*, 105-116.

[16] Nandari, W.W., Prasetyo, I. & Fahrurrozi, M. (2016). Optimasi Rasio Air dan Karbon Berpori untuk Proses Pembentukan Metana Hidrat. *Eksergi*, *13*(1), 17-20.

[17] Zakirova, G., Krapivsky, E., Berezovskaya, A., & Borisov, A. (2023). Storage of compressed natural gases. *Energies*, *16*(20), 7208. doi: 10.3390/en16207208.

[18] Ahammed, R. & Hasan, M.D.Z. (2023). An FEA and CFD coupled numerical analysis approach for characterizing magneto-rheological (MR) grease damper. https://doi.org/10.1007/s12046-023-02196-yS.

[19] Dharmanto, A., Muzakki, A.H., Sholih, H. & Domodite, A. (2025). Analysis of the strength of the frame construction on the nyamplung bean peeling machine using the finite element method. *TEKNOSAINS: Jurnal Sains, Teknologi dan Informatika, 12*(1), 1–7. https://doi.org/10.37373/tekno.v12i1.1027.

[20] Ishlah, N.W., Rega, S.J., Rohman, T. & Subekti, S. (2024). Analysis of air-to-water converter frame using ANSYS simulation. *JTTM: Jurnal Terapan Teknik Mesin, 5*(2), 274–279. https://doi.org/10.37373/jttm.v5i2.1125.

[21] Umashankar, M. & Santhosh, G.S. (2018). *Design of conical strainer and analysis using FEA*. www.ijesi.org

[22] Xie, X., Ma, L., Zhang, Q., Zhang, J., Dong, W. & Chen, R. (2024). Real-time finite element analysis based on surrogate model. *Journal of Physics: Conference Series, Institute of Physics*. https://doi.org/10.1088/1742-6596/2761/1/012036.

[23] Abuhatira, A.A., Salim, S.M. & Vorstius, J.B. (2023). CFD-FEA based model to predict leak-points in a 90-degree pipe elbow. *Engineering with Computers, 39*(6), 3941–3954. https://doi.org/10.1007/s00366-023-01853-4.

[24] Mumtaz Energy. (2024). *Temporary strainers*. https://wp123.mumtaz.com.my/products/temporary-strainers/.

[25] Saraçoğlu, M. H., Uslu, F., & Albayrak, U. (2021). Investigation of hole shape effect on static analysis of perforated plates with staggered holes. *International Journal of Engineering and Innovative Research*, *3*(2), 133-144. https://doi.org/10.47933/ijeir.883510.

[26] Pro Metall. *Perforated metal sheets: Perforation forms and perforation positions*.

[27] Rianto, R., Akhyan, A., Novison, R., Zaira, J.Y. & Haiqal, M. (2025). Studi numerik penurunan tekanan (dp) akibat perubahan sudut (theta), tipe lubang dan open rasio area (oar) pada strainer. *Jurnal Rekayasa Energi dan Mekanika*, *5*(1), 82.

[28] Colton Industries. *Temporary strainers* (pp. 1–2).

[29] Sobachkin, A. (2014). *Numerical basis of CAD-embedded CFD*.

[30] Wunda, S., Johanes, A.Z., Pingak, R.K. & Ahab, A.S. (2019). Tegangan regangan. *Fisika, 4*.

[31] Hayat, K.R. (2023). Analisis interaksi fluida dan struktur pada UAV STTA MALE generasi 1 dengan metode fluid structure interaction satu arah.

[32] Jia, L., Zhang, L., Guo, J., Yao, K., & He, S. (2018). Displacement and Stress Analysis of Thin Plate for Cement Concrete Pavement. *Mathematical Problems in Engineering*, *2018*(1), 3658540. doi: 10.1155/2018/3658540.

[33] Baron, K. & Sumner, D. (2025). Flow around surface-mounted low-aspect-ratio rectangular flat plates. *Fluid Dynamics Research*, 57, 035504. doi: 10.1088/1873-7005/ade285.

JOMAse | Received: 04-June-2025 | Accepted: 30-July-2025 | [(69) 2: 168-177]
Published by International Society of Ocean, Mechanical and Aerospace Scientists and Engineers, www.isomase.org., ISSN: 2354-7065 & e-ISSN: 2527-6085